PRAMANA
— journal of
physics

Vol. 85, No. 5
November 2015
pp. 993–1007

Soliton fission and supercontinuum generation in photonic crystal fibre for optical coherence tomography application

K PORSEZIAN[1,*] and R VASANTHA JAYAKANTHA RAJA[2]

[1]Department of Physics, Pondicherry University, Puducherry 605 014, India
[2]Centre for Nonlinear Science and Engineering, School of Electrical and Electronics Engineering, SASTRA University, Thanjavur 613 401, India
*Corresponding author. E-mail: ponzsol@yahoo.com

DOI: 10.1007/s12043-015-1114-5; ***e*Publication:** 17 October 2015

Abstract. We present a practical design of novel photonic crystal fibre (PCF) to investigate the nonlinear propagation of femtosecond pulses for the application of optical coherence tomography (OCT) based on supercontinuum generation (SCG) process. In addition, this paper contains a brief introduction of the physical phenomena of soliton and SCG. Typically, here we discuss how the ultrabroadband radiation in PCF can be generated by SCG through various nonlinear effects of the fibre. To accomplish the proposed aim, we put forth liquid core PCF (LCPCF) structure filled with chloroform for OCT measurements of the eye. From the proposed design, we observe that proposed LCPCFs with liquid material exhibit significant broadened wavelength spectrum with low input pulse energy over small propagation distances for the OCT application.

Keywords. Soliton fission; photonic crystal fibre; supercontinuum generation; optical coherence tomography.

PACS Nos 42.81.Qb; 42.65.Wi; 42.70.Jk; 42.65.Jx; 42.65.Pc; 82.35.Np

1. Introduction

Generation of broadband sources has always been of great interest as they find huge applications in many areas of science and technology. Supercontinuum generation (SCG), recognized in modern days as the 'white-light laser' process is found to be one of the best techniques to obtain broadband sources [1,2]. It has exceptional properties such as high brightness, a coherently pulsed nature, a high degree of spatial coherence, broad bandwidth and the requirement of low pulse energies. The phenomenon of supercontinuum (SC) has been achieved in different media such as solids, glasses, liquids, gases, etc., which manifest different kinds of structures [3]. These optical structures include electronic crystals, nanowires, photonic crystals, optical fibres, etc. Among these different structures, a special class of fibre called photonic crystal fibre (PCF) which is a lateral invention of the fibre structures, attract the researchers, as this kind of fibre has the capability of confining the light very tightly [3].

The increased interests in the study of the properties of the PCF are mainly due to their potential soliton-related applications in various nonlinear domains. The crucial advantages of soliton using PCF over conventional fibre are seen in many applications such as SCG, pulse compression, optical switching, fibre laser, parametric amplifier, modulational instability (MI), etc. [4–7]. Even though great deal of research has been carried out in PCF for various applications, generating broadband sources and ultrashort pulses using SCG technique finds wide applications in the modern and highly demanding technological world. With the rapid advancement in PCF technology, research on SCG has gained momentum and evolved as one of the most elegant and dramatic effects in optics with a wide range of potential applications in various fields such as frequency metrology, biomedical sensors, optical coherence tomography, wavelength division multiplexing, etc. [8–11].

SCG in a PCF was discovered by Ranka *et al* [12] as a means to generate a broad spectrum with two octave width at unprecedentedly low input pulse energies. Since then it has attracted extensive attention for both its fundamental and application aspects which was mainly motivated by its nonlinear applications. Already plenty of works have been demonstrated on SCG in PCF in all pump regimes ranging from continuous wave (CW), nanosecond, picosecond to femtosecond over the last decade. For instance, in the femtosecond regime, Nishizawa *et al* [13] reported a SC spectrum from 1100 to 2100 nm using a femtosecond fibre laser generating 110 fs pulses at 1550 nm. In parallel with these impressive results using femtosecond sources, there has been extensive continued interest in generating broadband SC by low-power picosecond and even nanosecond pulses. The combination of Raman scattering and four-wave mixing (FWM) was also observed in an experiment by Coen *et al* [14], where a pulse of 60 ps width with 40 nJ energy at 647 nm generated a 450 THz SC in the fundamental mode using 10 m of PCF with zero dispersion wavelength (ZDW) at 675 nm. This ensures that the Stokes and anti-Stokes bands generated by FWM directly from the pump to broaden and merge, resulting in a 600 nm wide SC source. In addition to femtosecond and picosecond regimes, a reasonable study on nanosecond pulse in SCG has also been reported using PCFs. Using 0.8 ns duration, 300 nJ energy pulses from a Q-switched microchip laser at 532 nm, Dudley *et al* [15] have generated SC from 460 to 750 nm over 250 THz of 1.8 m of PCF, through excitation of a higher-order mode whose ZDW at 580 nm was reached from the pump wavelength by cascaded Raman scattering. Then, the development of high-power CW fibre sources has also been applied to SCG. By using Yb^{3+}-doped fibre amplifier in a master oscillator power fibre amplifier at 1065 nm, Avodkhin *et al* [16] generated SC of 1065–1375 nm wavelength range with high-power CW fibre sources using 100 m long PCF. In addition to pulse duration, the effects of the input pulse parameters, such as pulse energy, peak power and central wavelength, on the SCG in PCF are subjects of high interest that have been thoroughly investigated.

Among the different techniques utilized by several authors to generate SC sources for various applications, obtaining broadband spectrum for optical coherence tomography (OCT) applications of the eye is the main theme of the present work. Even though broadband sources of central wavelength of 800 nm is optimal for OCT, it is difficult to produce such a broad source at near visible wavelength even from the best available laser sources. Of late, the generation of desired bandwidth of broadband source is quite possible using SC technique with the advent of PCF where the anomalous dispersion can also be obtained

at visible regime. As the application of SCG in OCT technology requires broadband and ultrashort pulses, it has been investigated through modelling PCF. The aim of this paper is not only to generate SCG for OCT applications, but also to study nonlinear phenomena of SCG in PCF. Hence, this paper is organized as follows: In the first part, nonlinear phenomena of soliton dynamics, soliton fission, role of higher-order linear and nonlinear effects and phenomena of SCG through PCF have been explained. In the second part, we intend to design PCF for the OCT application of eye.

2. Linear and nonlinear effects of the fibre

Among various nonlinear phenomena of the optical fibre, a key nonlinear process known as soliton plays an essential role in the SCG mechanism. When an optical pulse is transmitted, the various Fourier components will experience different indices of refraction in an optical fibre. As the refractive index is a measure of the velocity of the wave propagation in the optical fibre, different Fourier components travel with different velocity called the group velocity dispersion (GVD) or the chromatic dispersion. The group velocity parameter β_2 is given by

$$\beta_2 = \frac{\partial}{\partial\omega}\left(\frac{1}{v_g}\right) = -\frac{1}{v_g^2}\frac{\partial v_g}{\partial\omega}, \tag{1}$$

where v_g is the group velocity of the modulated wave. The pulse broadening is mainly due to GVD parameter β_2. The GVD varies with respect to wavelength λ. In order to account for the dispersion due to GVD, a useful parameter called dispersion length is defined in the following way:

$$L_D = \frac{T_0^2}{|\beta_2|}, \tag{2}$$

where T_0 is the pulse width. Figure 1 gives an idea about the broadening of pulse in a fibre due to GVD. The broadening of the pulse due to GVD will also add a chirp to the pulse. The chirp due to GVD will be either positive or negative depending on whether the fibre is of normal or anomalous dispersive type.

But for very intense light, the dielectric properties also depend on the intensity. This dependence is described by the nonlinear index n_2 by the relation $n = n_0 + n_2 I$, where $I = |E|^2$ [17]. This means that the phase velocity $v_p = c/n$ also becomes intensity-dependent. The pulse is therefore phase-modulated due to its own intensity profile. This

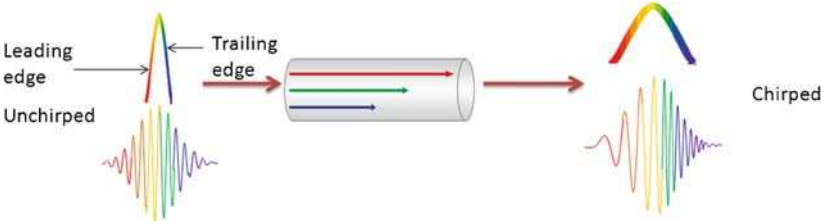

Figure 1. Different frequencies travel at different group velocities in fibre causing pulses to be chirped.

is referred to as self-phase modulation (SPM). Hence, SPM can be defined as the phase change of an optical pulse due to the self-induced change in the nonlinear refractive index. To illustrate the effects of SPM, the pulse propagation equation has been considered as [17]

$$\frac{\partial A}{\partial z} = \frac{i}{L_{\mathrm{NL}}} \exp(-2\alpha z)|A|^2 A. \tag{3}$$

Here, A is the normalized amplitude. The nonlinear length $L_{\mathrm{NL}} = 1/\gamma P_0$ provides the distance at which the nonlinear effects are important, where P_0 is the input power. The solution of eq. (3) is

$$A(z, T) = A(0, T) \exp[i\phi_{\mathrm{NL}}(z, T)] \tag{4}$$

with

$$\phi_{\mathrm{NL}}(z, T) = |A(0, T)|^2 \frac{z_{\mathrm{eff}}}{L_{\mathrm{NL}}}. \tag{5}$$

Here

$$z_{\mathrm{eff}} = \frac{1}{\alpha}[1 - \exp(-2\alpha z)] \tag{6}$$

and is smaller than z thus indicating that the loss limits the SPM. The time-dependent frequency shift induced by time-dependent phase ϕ_{NL} is given by

$$\delta\omega(T) = \frac{\partial |A(0, T)|^2}{\partial T} \frac{z_{\mathrm{eff}}}{L_{\mathrm{NL}}}. \tag{7}$$

The chirp is caused by SPM and increases in magnitude with the propagation. This chirp leads to negative frequency chirp on the leading edge of the pulse and positive frequency chirp on the trailing edge. Over a large central region, the chirp is almost linear and positive. Figure 2 shows the spectral evolution of SPM for an unchirped Gaussian input pulse.

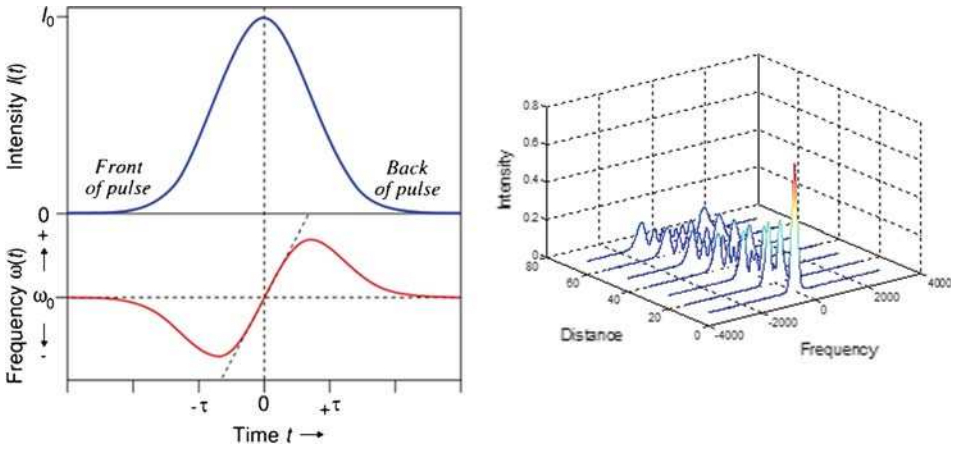

Figure 2. SPM acts as a positive chirp, which increases with increasing channel power level and system length (courtesy of google image).

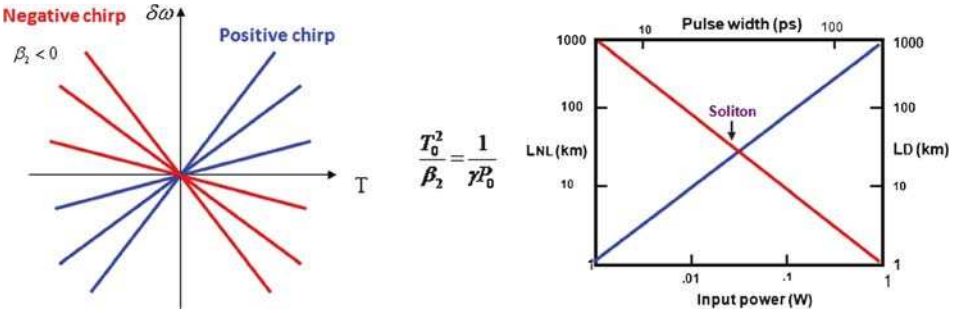

Figure 3. A condition can be obtained in which there is a perfect compensation of the effects. The GVD dispersion and nonlinear induced chirp have opposite signs (courtesy of google image).

Due to nonlinear temporal dependence of the chirp, the nonlinear phase-shift translates into broadening of the optical spectrum, generating new frequencies as the pulse travels inside the fibre. Also, it is observed that the slope of the frequency chirp increases with the distance. The temporal shape of the pulse remains unaffected.

3. Bright envelope solitons

The red-shifted part will propagate faster than blue-shifted part of the pulse in the case of normal dispersion regime. On the other hand, blue-shifted part will travel faster than the red-shifted part in the anomalous dispersion regime. The important thing to note is that if dispersion is anomalous and nonlinearity is present, the frequency chirps created by dispersion and SPM are opposite in nature. Hence, it is possible that the two chirps cancel giving chirp-free pulse when $L_{\mathrm{D}} = L_{\mathrm{NL}}$ as shown in figure 3. It turns out that it is possible for GVD and SPM to exactly balance each other. In this case neither the pulse nor its spectrum broadens. The undistorted pulse is called soliton [17]. Figure 4 shows the fundamental soliton evolution by balancing the chirp induced by anomalous GVD and SPM.

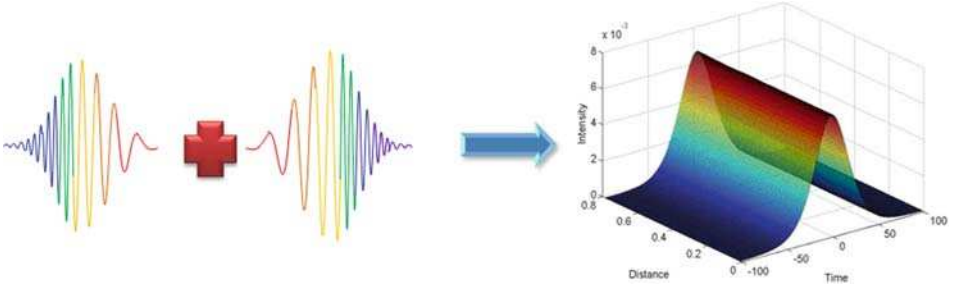

Figure 4. Formation of soliton by balancing the chirp induced by SPM and anomalous GVD.

Let us consider the propagation equation when only Kerr-like nonlinearity and second-order dispersion are included. Hence, the NLS equation can be written as [17]

$$\frac{\partial U}{\partial z} + \frac{i\beta_2}{2}\frac{\partial^2 U}{\partial T^2} = i\gamma(|U|^2 U), \tag{8}$$

where U is the slowly-varying envelope of the wave, z is the longitudinal coordinate and t is the time in the moving reference frame. The Kerr nonlinear coefficient γ is calculated using the formula $\gamma = n_2\omega_0/cA_{\text{eff}}$, where c is the velocity of light. The fundamental soliton solution to this equation can be obtained directly by assuming a shape-preserving solution of the form $U(z, T) = V(T)\exp[i\phi(z, T)]$. The result is [17]

$$U(z, T) = \sqrt{(}P_0)\ \text{sech}\left(\frac{T}{T_0}\right)\exp\left[\frac{i|\beta_2|}{2T_0^2}z\right] \tag{9}$$

with $N = 1$, where

$$N^2 = \frac{\gamma P_0 T_0^2}{|\beta_2|}. \tag{10}$$

Here, N is the soliton order. In the context of optical fibres, the solution (9) indicates that if a hyperbolic secant pulse, whose width T_0 and the peak power P_0 are chosen such that $N = 1$ in eq. (10), is launched inside an ideal lossless fibre, the pulse will propagate without change in shape for arbitrarily long distances. This is the unique feature of the fundamental solitons that makes them attractive for optical communication systems [17]. The peak power P_0 required to support the fundamental soliton is obtained from eq. (10) by setting $N = 1$ and is given by

$$P_0 = \frac{|\beta_2|}{\gamma T_0^2}. \tag{11}$$

For single soliton pulse propagation, the hyperbolic secant shape is preserved for very long distance. For integer values of N larger than 1, a higher-order soliton is formed which does not preserve its shape during propagation. Instead, such waves follow a periodic evolution during propagation with shape recovering at multiples of the soliton period defined as $\pi/2L_{\text{D}}$. This basic phenomenon of soliton plays a major role in SCG in achieving broadband spectra and ultrashort pulse.

4. Raman effect

When a light wave is incident on a fibre at the carrier frequency ω_0 in the presence of some resonance level ω_{R} of the fibre material, the incident light results in the downshift of the carrier frequency, resulting in an entirely new frequency $\omega_0 - \omega_{\text{R}}$, known as the mode frequency. Such a process is known as Raman effect [17]. The principle of Raman scattering is that a lower wavelength pump-laser light travelling down an optical fibre along with the signal, scatters off atoms in the fibre, losses some energy to the atoms, and then continues its journey with the same wavelength as the signal. Therefore, the signal has additional photons representing it and, hence, is amplified. This new photon can now be joined by many more from the pump, which continue to be scattered as they travel

down the fibre in a cascading process. When the frequency beating between the incident and scattered waves collectively enhances the optical photon, the scattering process is stimulated and the amplitude of the scattered wave grows exponentially in the direction of propagation, a phenomenon known as the stimulated Raman scattering (SRS). For solitons, this effect shifts the soliton spectrum towards lower frequencies which is called self-frequency shift.

5. Mechanism of SCG

The detailed physical aspects of SCG can be interpreted by means of interplay of various nonlinear effects like SPM, Raman scattering and four-wave mixing (FWM). Among the various nonlinear phenomena, soliton forms the base for SCG mechanism. A complete theory of SCG by using soliton-related effects was proposed by Husakou *et al* [18], which has been confirmed by experiments and numerical simulations in the femtosecond regime [19]. Among the soliton-related effects, the two vital aspects of high degree of importance, namely, the soliton frequency shift induced by the Raman scattering and emission of dispersive radiation due to third-order dispersion, play crucial roles in SCG (figure 5).

A conceptually clear way to understand the main features of SCG in the femtosecond regime is to first consider the case of pumping in the anomalous dispersion regime, but close to the fibre's ZDW. Under typical pumping conditions, the power of the pump pulses is high enough for the input pulses to be considered as soliton of order N. A higher-order soliton pulse N breaks up into N constituent red-shifted solitons with varying group velocities. In principle, the energy of the fundamental soliton does not change, but it emits spectral components on the shorter wavelength (anti-Stokes) side of the pulse spectrum. The existence of such blue-shifted radiation is known as nonsolitonic radiation (NSR), also called dispersive radiation. The wavelength of the NSR is determined by phase matching condition as a result of perturbation by third- and higher-order dispersion.

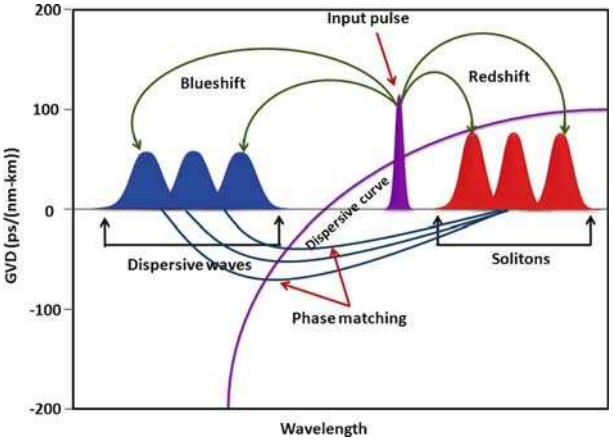

Figure 5. Scheme of a SCG by fission of higher-order solitons. Thick violet line is GVD for a PCF. Spectra of NSR, solitons and input pulse are presented by blue, red and violet colour pulses, respectively. The phase mismatch between solitons and NSR is presented by blue lines.

The phases of non-solitonic radiation at ω_d and soliton at frequency ω_s at a distance z after a delay $T = z/v_g$ are given by [17]

$$\phi_{\omega_d} = \beta(\omega_d)z - \omega_d(z/v_g), \tag{12}$$

$$\phi_{\omega_s} = \beta(\omega_s)z - \omega_s(z/v_g) + \frac{1}{2}\gamma P_s z, \tag{13}$$

where P_s is the peak power of the Raman soliton formed after fission process. The last term in eq. (13) represents nonlinear phase shift due to soliton. As the central frequency ω_s of the solition changes because of a Raman-induced frequency shift, the frequency of the dispersive wave would also change. If we expand $\beta(\omega_d)$ in Taylor series around ω_s, the two phases are matched when the frequency shift $\Omega_d = \omega_d - \omega_s$ satisfies

$$\sum_{n=2}^{\infty} \frac{\beta_n(\omega_s)}{n!}\Omega_d^n = \frac{1}{2}\gamma P_s. \tag{14}$$

It is easy to see from eq. (14) that Ω_d will not have any solution if the higher-order dispersive terms are absent and $\beta_2 < 0$. However, if we include the TOD, the resulting cubic polynomial, $\beta_3\Omega_d^3 + 3\beta_2\Omega_d^2 - 3\gamma P_s = 0$, provides the following approximate solution:

$$\Omega_d \approx -\frac{3\beta_2}{\beta_3} + \frac{\gamma P_s \beta_3}{3\beta_2^2}. \tag{15}$$

For soliton propagation in the anomalous dispersion regime such that $\beta_2 < 0$ and $\beta_3 > 0$, the frequency shift Ω_d is positive. As a result, the NSR is emitted at a higher frequency (or a shorter wavelength) than that of the soliton. This situation changes in fibres with $\beta_3 < 0$ for which the NSR can be emitted at wavelengths longer than that of the soliton. In a PCF, higher-order dispersion effects are stronger than in standard fibres and play a much more significant role in pulse propagation. In PCFs, the generation of multiple frequency components due to soliton fission in the presence of Raman effect and third-order dispersion is much more pronounced. The distinct spectral fractions arise due to the existence of multisolitons with different frequencies, results in a broad spectrum as a consequence of nonlinear interactions between soliton and blue-shifted continuum.

6. Optical coherence tomography

OCT is an emerging biomedical image technique. Obtaining micrometer scale fine spatial resolution cross-sectional images of the highly scattering media, portability and cost effectiveness are main advantages of SCG in OCT. By using OCT technique one can obtain high-resolution cross-sectional image without physically damaging the tissue. The penetration depth of the OCT is typically limited by optical scattering of the tissue. The optimal choice of the centre wavelength depends on the biological medium under investigation. To achieve a good penetration depth, the 800 nm wavelength region is optimal for OCT measurements of the eye, due to lower absorption, while the 1300 nm region is considered optimal for the measurements of highly scattering tissue such as skin, due to lower scattering. For instance, Kawagoe *et al* [20] developed a high power SC source at a centre wavelength of 1.7 μm to demonstrate highly penetrative ultrahigh-resolution

OCT. Aguirre *et al* [21] demonstared high resolution OCT at 800 nm and 1300 nm using SCG in a single PCF with a parabolic dispersion profile and two closely spaced ZDW. By doping germanium, which has higher refractive index, inside the host silica, Hossain *et al* [22] proposed novel PCF to generate SC radiation for dental OCT applications at 1.31 μm. The novel PCFs were also proposed for dental optical diagnostics in [23,24]. The generation of broadband laser pulses at shorter wavelength near 800 nm is especially preferred in OCT measurement of the eye [25].

It is desirable to have an OCT light source with a spectrum that is extremely broad (hundreds of nanometres), relatively smooth and flat, and a centre wavelength adjusted to the particular OCT application. Due to the interferometric basis of the technique, the resolution depth Δz of the cross-sectional image is related to the centre wavelength λ_c and the FWHM bandwidth $\Delta\lambda$ of the light source as [26]

$$\Delta z = \frac{2\ln 2}{\pi}\frac{\lambda_c^2}{\Delta\lambda} \approx 0.44\frac{\lambda_c^2}{\Delta\lambda}. \tag{16}$$

7. Designing PCF for the OCT measurement of the eye

In order to compare the quality of the proposed PCF, we first design the silica core PCF and then study the dynamics of the SC pulse. We start the analysis to design the conventional PCF at 800 nm with large air hole diameter (d) and small pitch (Λ) constant to achieve large dispersion and high nonlinearity values. However, it is noteworthy that, after attaining certain value of normalized air-hole size (d/Λ), the fibre may not be a single mode at 800 nm. Hence, to study the SC at 800 nm, we design the conventional silica core PCF with structure parameters of $d/\Lambda = 0.65$ and $\Lambda = 1$ μm. To understand the dynamics of ultrashort pulse propagation in the proposed PCF, we have used the modified nonlinear Schrödinger (MNLS) equation of the following form [3]:

$$\frac{\partial U}{\partial z} + \sum_{n=2}^{4}\beta_n\frac{i^{n-1}}{n!}\frac{\partial^n U}{\partial t^n} = i\gamma\left(1+\tau_{\text{shock}}\frac{\partial}{\partial t}\right) \times\left(U\int_{-\infty}^{t}R(\tau)|U(t-\tau)|^2\mathrm{d}\tau\right). \tag{17}$$

The parameters β_n are the $n\,(=2,3,4)$th-order dispersion coefficient. The response function of $R(t)$ can be written as

$$R(t) = (1-f_R)\delta(t) + f_R h_R(t), \tag{18}$$

where f_R represents the fractional contribution of the delayed Raman response (0.18 for silica and 0.35 for chloroform) and h_R is the Raman response function. To investigate the SCG in PCF, we numerically solve eq. (17) using split step Fourier method (SSFM) with initial envelope of the soliton for the peak power $P_0 = 20$ kW at $z = 0$ given by $U(0,t) = \sqrt{P_0}\,\mathrm{sech}(t)$. Numerical simulation is carried out for the input pulse by setting wavelength $\lambda = 800$ nm and the pulse width FWHM of 20 fs. The fibre parameters are evaluated using the fully vectorial effective index method which is a widely used numerical technique that provides the propagation constant of the guided modes in PCF [27], with the wavelength

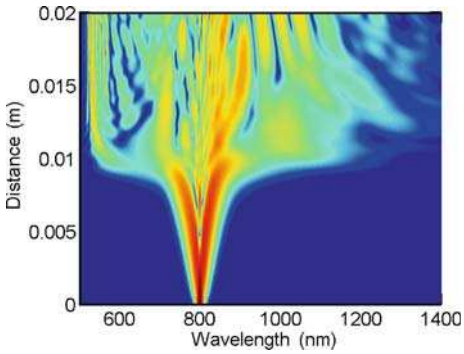

Figure 6. The SCG for 20 fs input pulse width in silica core PCF at 800 nm. The fibre parameters are $\beta_2 = -0.0148883$ ps^2/m, $\beta_3 = 0.000032771$ ps^3/m and $\beta_4 = 1.19 \times 10^{-7}$ps^4/m. The nonlinearity value $\gamma = 0.04869$ W^{-1} m^{-1}. The propagation length $L = 2$ cm.

dependence of the refractive index of silica included in the dispersion calculation. The fibre parameters are $\beta_2 = -0.0148883$ ps^2/m, $\beta_3 = 0.000032771$ ps^3/m and $\beta_4 = 1.19 \times 10^{-7}$ ps^4/m and the nonlinearity value is $\gamma = 0.04869$ W^{-1} m^{-1} for PCF. Figure 6 shows the spectral evolution of SC pulse in PCF. Simultaneously, we have also analysed the evolution of soliton dynamics in the time domain from figure 7. From these two figures we come to the conclusion that high input power is required to obtain the SC pulse in silica core PCF. Hence, we anticipate another PCF to minimize input power as low as possible.

8. SCG in non-silica PCF

In general, there are two proven ways to enhance the nonlinearity and dispersion values in PCFs. First, one can modify the design of PCF with large air hole size leading

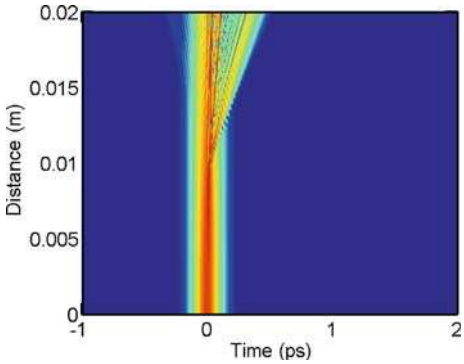

Figure 7. The pulse propagation through silica core PCF. The fibre parameters are $\beta_2 = -0.0148883$ ps^2/m, $\beta_3 = 0.000032771$ ps^3/m and $\beta_4 = 1.19 \times 10^{-7}$ ps^4/m. The nonlinearity value $\gamma = 0.04869$ W^{-1} m^{-1}. The propagation length $L = 2$ cm.

to high nonlinearity and large dispersion. However, the single mode tends to vanish for larger values of air hole size. Secondly, the non-silica technology such as SF6, TF10, CS_2, nitrobenzene etc., enhances the nonlinearity and eventually the required input energy of the pulse can be minimized considerably [28–30]. For instance, Zhang *et al* [31] utilized the liquid core PCF (LCPCF) with CS_2 and nitrobenzene filled into the core to generate dramatically broadened SC in a range from 700nm to more than 2500 nm when pumped at 1.55 μm with subpicosecond pulses. Our group also studied the nonlinear optical phenomena with ultrabroadband radiation in LCPCF. Since the LCPCF has complex nonlinear phenomena, we analysed the role of saturable nonlinear response and slow nonlinear response on SCG in detail [32,33]. There has been an increasing interest in another type of PCF made of softglass for mid-infrared SCG due to its higher nonlinearity and low transmission loss in the mid-infrared region 2–4 μm [34]. For example, an SC with a bandwidth exceeding 4 μm was generated in a short tellurite fibre by using 110 fs pulses at 1550 nm [34]. Additionally, in a recent experiment, a centimetre-long ZBLAN fluoride fibre was pumped in the normal dispersion regime by a 1450 nm femtosecond laser and despite having nonlinearity comparable to silica, an ultrabroad SC spanning from the ultraviolet to $\sim$6 μm was demonstrated [35]. In parallel, Ole Bang *et al* demonstrated the formation of SCG in tellurite PCFs specially designed for high power picosecond pumping at the thulium wavelength of 1930 nm [36].

Even in the non-silica technology, obtaining anomalous dispersion at visible regime is very difficult in PCF for large air hole diameter. Nevertheless, one can achieve all the required parameters such as large values of dispersion and nonlinearity by filling the chloroform liquid in the core region of the PCF [37]. SCG in chloroform-filled LCPCF has also been demonstrated at 800 nm in [37]. Based on this work, we have designed novel PCF structures for efficient soliton propagation and pulse compression in chloroform-filled LCPCF [38,39]. The existence of anomalous dispersion in this highly nonlinear PCF near visible wavelength brings the attention that the broadband pulse can be attained using SC technique for OCT measurement of the eye.

9. Designing novel PCF for OCT

At the outset, we intend to design highly nonlinear PCF for the investigation of the eye using OCT technique. As the aim of the present work is to achieve the SC at very short distance with low input power, we would like to try another design of PCF. Since liquid chloroform has very high nonlinearity and the refractive index is almost equal to that of silica, we consider the PCF with chloroform filled in the core region as shown in figure 8. The value of nonlinear coefficient n_2 of chloroform is 1.7×10^{-18} m^2/W and the refractive index of chloroform is given by [39]

$$n_{\mathrm{CHCl_3}} = 1.431364 + 5632.41 \times \lambda^{-2} - 2.0805 \times 10^{8} \times \lambda^{-4} + 1.2613 \times 10^{13} \times \lambda^{-6}, \tag{19}$$

where λ is the wavelength in nm. The newly designed chloroform-filled LCPCF offers low dispersion and nonlinear length scales when appropriate PCF parameters are chosen. The modified LCPCF has $d_c/\Lambda_c = 0.85$ with $\Lambda_c = 1.1$ μm and the core diameter D is equal to the diameter of air-hole in the outer ring d_c, i.e. $D = d_c$. The variation of GVD

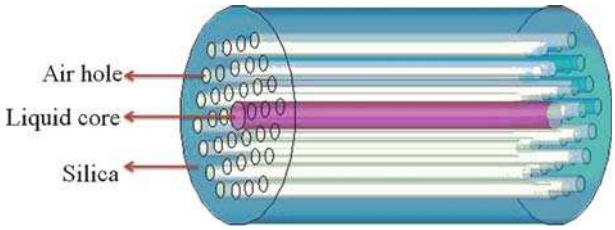

Figure 8. Schematic diagram of liquid-filled PCF.

parameters as a function of wavelength is represented in figure 9. In order to compare the efficiency of the SC sources in the proposed PCF, we have started our discussion from designing fibre with the same dispersion parameter value for both the conventional silica as well as the proposed LCPCF.

To investigate the dynamical behaviour of the SC in the newly designed chloroform-filled LCPCF, we consider the same length as in the case of the conventional PCF. The pulse parameter values are maintained the same for both the designed LCPCF and the conventional PCF. The required input power and length of the PCF can be calculated from the dispersion and nonlinear length scales. Since the nonlinearity of CPCF is almost 200 times larger than the SPCF, it is clear that CPCF can attain the same broadening with an input power 200 times lower than that of the SPCF. This is confirmed by the numerical simulation that SC is obtained at the pulse power of 20 kW and 200 W for fibre design PCF and LCPCF, respectively. Figure 10 illustrates the dynamics of SC pulse for the newly proposed LCPCF. The corresponding soliton breaking dynamics is shown in figure 11. It is fascinating to observe from figure 6 that the dispersive wave components emerge at shorter distance of pulse propagation with low power, overwhelming the fact that the nonlinear and dispersion value of chloroform-filled LCPCF are very large in comparison to the ordinary solid core PCF. Thus, one can achieve efficient broad spectrum typically SC pulse at 800 nm for OCT application using low input power in chloroform-filled LCPCF rather than in silica core PCF .

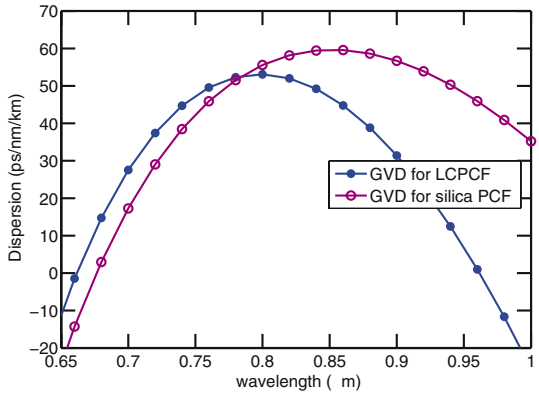

Figure 9. The variation of GVD for different wavelengths for both SPCF and LCPCF.

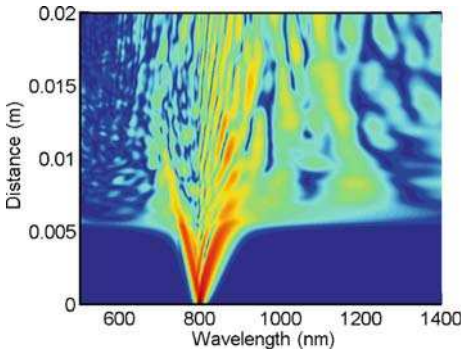

Figure 10. The SCG for 20 fs input pulse width in LCPCF at 800 nm. The fibre parameters are $\beta_2 = -0.018$ ps^2/m, $\beta_3 = 0.000004850570$ ps^3/m and $\beta_4 = 7.059 \times 10^{-7}$ ps^4/m. The nonlinearity value $\gamma = 14.56$ W^{-1} m^{-1}. The propagation length $L = 2$ cm.

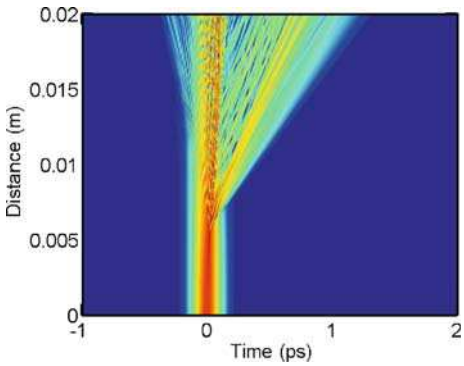

Figure 11. The pulse propagation through LCPCF. The fibre parameters are $\beta_2 = -0.018$ ps^2/m, $\beta_3 = 0.000004850570$ ps^3/m and $\beta_4 = 7.059 \times 10^{-7}$ ps^4/m. The nonlinearity value $\gamma = 14.56$ W^{-1} m^{-1}. The propagation length $L = 2$ cm.

10. Conclusion

In conclusion, we have theoretically investigated the nonlinear propagation of femtosecond pulses in PCF. The detailed physical aspects of soliton fission and broadband SCG dynamics have been studied using appropriately modified NLS equation by means of interplay between various nonlinear effects like SPM, Raman scattering and higher-order dispersion in the femtosecond regime. To achieve broadband pulse using SCG technique for OCT application of the eye, we have first numerically investigated the dynamics of soliton propagation at 800 nm in silica core PCF. Subsequently, we have successfully investigated the novel theoretical design of chloroform-filled PCF to achieve SC pulse-with low input power for OCT applications of the eye. It has been observed that one can achieve high resolution depth in novel PCF at very short length with low input energy at 800 nm in contrast to silica core PCF.

Acknowledgement

KP acknowledges DST, IFCPAR, NBHM, DST-FCI and CSIR, the Government of India for financial support through major projects. RVJR wishes to thank DST fast-track programme for providing financial support.

References

[1] A M Zheltikov, *Physics-Uspekhi* **49(6)**, 605 (2006)
[2] D V Skryabin and A V Gorbach, *Rev. Mod. Phys.* **82**, 1287 (2010)
[3] J M Dudley and J R Taylor (Eds) *Optical fiber supercontinuum generation*, 1st edn (Cambridge University Press, Cambridge, 2010)
[4] F W Wise, A Chong and W H Renninger, *Laser Photon. Rev.* **2**, 58 (2008)
[5] T Uthayakumar, R Vasantha Jayakantha Raja and K Porsezian, *Opt. Commun.* **296**, 124 (2013)
[6] M H Frosz, T Sørensen and O Bang, *J. Opt. Soc. Am. B* **23**, 1692 (2006)
[7] A K Sarma, *Jpn. J. Appl. Phys.* **47**, 5493 (2008)
[8] J H V Price, K Furusawa, T M Monro, L Lefort and D J Richardson, *J. Opt. Soc. Am. B* **19**, 1286 (2002)
[9] N I Nikolov, T Sørensen, O Bang and A Bjarklev, *J. Opt. Soc. Am. B* **20**, 2329 (2003)
[10] A V Avdokhin, S V Popov and J R Taylor, *Opt. Lett.* **28**, 1353 (2003)
[11] J M Dudley, G Genty and S Coen, *Rev. Mod. Phys.* **78**, 1135 (2006)
[12] J K Ranka, R S Windeler and A J Stentz, *Opt. Lett.* **25**, 25 (2000)
[13] N Nishizawa, Y Chen, P Hsiung, E P Ippen and J G Fujimoto, *Opt. Lett.* **29**, 2846 (2004)
[14] S Coen, A H Chau, R Leonhardt, J D Harvey, J C Knight, W J Wadsworth and P St J Russell, *J. Opt. Soc. Am. B* **19**, 753 (2002)
[15] J M Dudley, L Provino, N Grossard, H Maillotte, R S Windeler, B J Eggleton and S Coen, *J. Opt. Soc. Am. B* **19**, 765 (2002)
[16] A V Avdokhin, S V Popov and J R Taylor, *Opt. Lett.* **28**, 1353 (2003)
[17] G P Agrawal, *Nonlinear fiber optics* (Academic Press, 2001)
[18] A V Husakou and J Herrmann, *Phys. Rev. Lett.* **87**, 203901 (2001)
[19] J Herrmann, U Griebner, N Zhavoronkov, A Husakou, W J Wadsworth, J C Knight, P St J Russell and G Korn, *Phys. Rev. Lett.* **88**, 173901 (2002)
[20] H Kawagoe, S Ishida, M Aramaki, Y Sakakibara, E Omoda, H Kataura and N Nishizawa, *Bio. Opt. Express* **5**, 932 (2014)
[21] A D Aguirre, N Nishizawa, J G Fujimoto, W Seitz, M Lederer and D Kopf, *Opt. Express* **14**, 1145 (2006)
[22] M A Hossain, Y Namihira, S M A Razzak, M A Islam, J Liu, S F Kaijage and Y Hirako, *Opt. Laser Tech.* **44**, 976 (2012)
[23] Y Namihira, M A Hossain, T Koga, M A Islam, S M A Razzak, S F Kaijage, Y Hirako and H Higa, *Opt. Rev.* **19**, 78 (2012)
[24] S O Konorov, V P Mitrokhin, A B Fedotov, D A S Biryukov, V I Beloglazov, N B Skibina, A V Shcherbakov, E Wintner, M Scalora and A M Zheltikov, *Appl. Opt.* **43**, 2251 (2004)
[25] S W Lee, H W Song, B K Kim, M Y Jung, S H Kim, J D Cho and C S Kim, *J. Opt. Soc. Korea* **15**, 293 (2011)
[26] I Hartl, X D Li, C Chudoba, R K Ghanta, T H Ko, J G Fujimoto, J K Ranka and R S Windeler, *Opt. Lett.* **26**, 608 (2001)

[27] R Vasantha Jayakantha Raja and K Porsezian, *J. Photon. Nanostruct. – Fundamentals and Applications* **5**, 171 (2007)
[28] M Vieweg, T Gissibl, S Pricking, B T Kuhlmey, D C Wu, B J Eggleton and H Giessen, *Opt. Express* **18**, 25232 (2010)
[29] S Yiou, P Delaye, A Rouvie, J Chinaud, R Frey and G Roosen, *Opt. Express* **13**, 4786 (2005)
[30] C J S de Matos, C M B Cordeiro, M E dos Santos, J S K Ong, A Bozolan and C H B Cruz, *Opt. Express* **15**, 11207 (2007)
[31] R Zhang, J Teipel and H Giessen, *Opt. Express* **14**, 6800 (2006)
[32] R Vasantha Jayakantha Raja, K Porsezian and K Nithyanandan, *Phys. Rev. A* **82**, 013825 (2010)
[33] R Vasantha Jayakantha Raja, A Husakou, J Hermann and K Porsezian, *J. Opt. Soc. Am. B* **27**, 1763 (2010)
[34] P Domachuk, N A Wolchover, M Cronin-Golomb, A Wang, A K George, C M B Cordeiro, J C Knight and F G Omenetto, *Opt. Express* **16**, 7161 (2008)
[35] G Qin, X Yan, C Kito, M Liao, T Suzuki, A Mori and Y Ohishi, *Appl. Phys. Lett.* **95**, 161103 (2009)
[36] D Buccoliero, H Steffensen, O Bang, H E Heidepriem and T M Monro, *Appl. Phys. Lett.* **97**, 061106 (2010)
[37] H Zhang, S Chang, J Yuan and D Huang, *Optik* **121**, 783 (2010)
[38] R Vasantha Jayakantha Raja, K Senthilnathan, K Porsezian and K Nakkeeran, *IEEE – J. Quant. Elect.* **46**, 1795 (2010)
[39] R Vasantha Jayakantha Raja, K Porsezian, Shailendra K Varshney and S Sivabalan, *Opt. Commun.* **283**, 5000 (2010)